

Technical Appendix to Doh (2010) “Yield Curve in an Estimated Nonlinear Macro Model”

Taeyoung Doh

October 15, 2010

1 Derivation of Equilibrium Bond Yields

All the notations are the same as the paper. The coefficients on $\hat{p}_{1,t}$ are obtained by the policy function for the nominal interest rate because $\hat{p}_{1,t} = -\widehat{(1+i_t)}$. To derive coefficients of long-term bond yields recursively, I use the following expressions,

$$\begin{aligned}
 a_1 &= -g_{\sigma\sigma}^i, \quad b_1 = -g_x^i, \quad c_1 = -g_{xx}^i, \\
 \hat{M}_{t,t+1} &= (\hat{\lambda}_{t+1}^a - \hat{\lambda}_t^a) - \hat{u}_{a,t+1} - \hat{\pi}_{t+1}, \\
 \hat{M}_{t,t+1} + \hat{p}_{n-1,t+1} &= x'_{t+1} \left(\frac{1}{2} g_{xx}^{\lambda^a} - \frac{1}{2} g_{xx}^{\pi} + c_{n-1} \right) x_{t+1} + (g_x^{\lambda^a} - b_a - g_x^{\pi} + b_{n-1}) x_{t+1} \\
 &+ x'_t \left(-\frac{1}{2} g_{xx}^{\lambda^a} \right) x_t - g_x^{\lambda^a} x_t - \frac{1}{2} g_{\sigma\sigma}^{\pi} + a_{n-1}, \\
 &= x'_{t+1} \Omega_0 x_{t+1} + \Omega_1 x_{t+1} + \Omega_2,
 \end{aligned} \tag{1}$$

where $b_a = [1, 0, \dots, 0] (1 \times n_x)$.

If x_t contains only exogenous shocks that follow linear processes, the above expression would only contain second-order terms at with respect to (x_t, ϵ_{t+1}) . However, x_t contains lagged endogenous variables, such as the past interest rate and the past consumption, that follow quadratic transition equations. Therefore, the above expression for $\hat{M}_{t,t+1} + \hat{p}_{n-1,t+1}$ should also include higher than second-order terms with respect to (x_t, ϵ_{t+1}) . Since these extra higher-order terms do not, in general, increase the accuracy of approximation, and may induce explosive behavior at long horizons, as shown in Kim et. al. (2008), I eliminate them and use the following approximate expressions for $\hat{M}_{t,t+1} + \hat{p}_{n-1,t+1}$ to derive equilibrium bond yields,

$$\begin{aligned}
 x'_{t+1} \Omega_0 x_{t+1} &= (\Gamma_1 x_t + \eta \epsilon_{t+1})' \Omega_0 (\Gamma_1 x_t + \eta \epsilon_{t+1}) + o_p(\sigma^2), \\
 &\approx x'_t (\Gamma_1' \Omega_0 \Gamma_1) x_t + 2x'_t \Gamma_1' \Omega_0 \eta \epsilon_{t+1} + \epsilon'_{t+1} \eta' \Omega_0 \eta \epsilon_{t+1}, \\
 \Omega_1 x_{t+1} &= \Omega_1 (\Gamma_0 + \Gamma_1 x_t + (I_{n_x} \otimes x_t)' \Gamma_2 x_t + \eta \epsilon_{t+1}) + o_p(\sigma^2), \\
 &\approx \Omega_1 (\Gamma_0 + \Gamma_1 x_t + (I_{n_x} \otimes x_t)' \Gamma_2 x_t + \eta \epsilon_{t+1}), \\
 \Omega_2 &= x'_t \left(-\frac{1}{2} g_{xx}^{\lambda^a} \right) x_t - g_x^{\lambda^a} x_t - \frac{1}{2} g_{\sigma\sigma}^{\pi} + a_{n-1}.
 \end{aligned} \tag{2}$$

Rearranging the approximated $\hat{M}_{t,t+1} + \hat{p}_{n-1,t+1}$ by the order of ϵ_{t+1} leads to the following equation,

$$\begin{aligned}
\hat{M}_{t,t+1} + \hat{p}_{n-1,t+1} &\approx \epsilon'_{t+1} C_{n-1} \epsilon_{t+1} + B_{n-1} \epsilon_{t+1} + A_{n-1}, \\
\text{In the end, } C_{n-1} &= \eta' \Omega_0 \eta, \quad B_{n-1} = 2x'_t \Gamma'_1 \Omega_0 \eta + \Omega_1 \eta, \\
\text{where, } A_{n-1} &= x'_t (\Gamma'_1 \Omega_0 \Gamma_1 - \frac{1}{2} g_{xx}^{\lambda^a}) x_t + \Omega_1 (I_{n_x} \otimes x_t)' \Gamma_2 x_t \\
&\quad + \Omega_1 (\Gamma_0 + \Gamma_1 x_t) - g_x^\lambda x_t - \frac{1}{2} g_{\sigma\sigma}^\pi + a_{n-1}. \tag{3}
\end{aligned}$$

Now, I use the multi-normality of ϵ_{t+1} to compute conditional expectations in no-arbitrage conditions,

$$\begin{aligned}
&E_t(e^{\epsilon'_{t+1} C_{n-1} \epsilon_{t+1} + B_{n-1} \epsilon_{t+1} + A_{n-1}}), = \int |2\pi I|^{-\frac{1}{2}} e^{(-\frac{1}{2} \epsilon'_{t+1} (I - 2C_{n-1}) \epsilon_{t+1} + B_{n-1} \epsilon_{t+1} + A_{n-1})} d\epsilon_{t+1}, \\
&= \int |2\pi (I - 2C_{n-1})|^{-\frac{1}{2}} e^{(-\frac{1}{2} \epsilon'_{t+1} (I - 2C_{n-1}) \epsilon_{t+1})} \times e^{(B_{n-1} \epsilon_{t+1})} |I - 2C_{n-1}|^{-\frac{1}{2}} e^{A_{n-1}} d\epsilon_{t+1}, \\
&= \int |2\pi (I - 2C_{n-1})|^{-\frac{1}{2}} e^{(-\frac{1}{2} (\epsilon_{t+1} - (I - 2C_{n-1})^{-1} B'_{n-1})' (I - 2C_{n-1}) (\epsilon_{t+1} - (I - 2C_{n-1})^{-1} B'_{n-1}))} \\
&\quad \times e^{(B_{n-1} (I - 2C_{n-1})^{-1} B'_{n-1})} |I - 2C_{n-1}|^{-\frac{1}{2}} e^{A_{n-1}} d\epsilon_{t+1}, \\
&= e^{\frac{1}{2} B_{n-1} (I - 2C_{n-1})^{-1} B'_{n-1}} |I - 2C_{n-1}|^{-\frac{1}{2}} e^{A_{n-1}}, \quad \epsilon_{t+1} \sim \mathcal{N}(0, I). \tag{4}
\end{aligned}$$

As long as $I - 2C_{n-1}$ is positive definite, this expression is well defined. Practically, C_{n-1} is quite small relative to I and this condition is satisfied for all the prior and posterior draws. By matching $\frac{1}{2} B_{n-1} (I - 2C_{n-1})^{-1} B'_{n-1} - \frac{1}{2} \ln |I - 2C_{n-1}| + A_{n-1}$ with $a_n + b_n x_t + x'_t c_n x_t$, the following recursive formulas for the coefficients are obtained,

$$\begin{aligned}
a_n &= a_{n-1} + \Omega_1 \Gamma_0 + \frac{1}{2} \Omega_1 \eta (I - 2C_{n-1})^{-1} \eta' \Omega'_1 - \frac{1}{2} g_{\sigma\sigma}^\pi - \frac{1}{2} \ln |I - 2C_{n-1}|, \\
b_n &= -g_x^{\lambda^a} + \Omega_1 \Gamma_1 + 2\Omega_1 \eta (I - 2C_{n-1})^{-1} \eta' \Omega'_0 \Gamma_1, \\
c_n &= 2\Gamma'_1 \Omega_0 \eta (I - 2C_{n-1})^{-1} \eta' \Omega'_0 \Gamma_1 + \Gamma'_1 \Omega_0 \Gamma_1 - \frac{1}{2} g_{xx}^{\lambda^a} \\
&\quad + [(g_x^{\lambda^a} - b_a - g_x^\pi + b_{n-1})]_{i_{t-1}} [\Gamma_2]_{i_{t-1}} \\
&\quad + [(g_x^{\lambda^a} - b_a - g_x^\pi + b_{n-1})]_{c_{t-1}} [\Gamma_2]_{c_{t-1}}. \tag{5}
\end{aligned}$$

Here the subscripts (i_{t-1}, c_{t-1}) denote the element or the matrix related to these variables. The above-mentioned recursive formulas extend recursive formulas for coefficients in the affine term structure model. If I consider only the first-order terms and adjust the risk premium by the conditional variance of first-order terms, the following affine recursion formulas can be applied,

$$\begin{aligned}
a_n &= a_{n-1} + \frac{1}{2} \Omega_1 \eta \eta' \Omega'_1, \\
b_n &= -g_x^{\lambda^a} + \Omega_1 \Gamma_1, \\
\text{where } a_0 &= 0, \quad b_0 = [0, \dots, 0]. \tag{6}
\end{aligned}$$

2 Alternative methods of computing equilibrium bond yields in a nonlinear model

There are alternative methods of computing equilibrium bond yields implied by a DSGE model solved with a higher-order approximation. For example, Ravenna and Seppälä (2006) suggest running nonlinear regressions of the simulated pricing kernel on state variables to obtain equilibrium bond prices as follows,

$$e^{\sum_{j=1}^J m_{t,t+j}^i} = a_j + b_j x_t + x_t' c_j x_t + u_{j,t}^i, \quad i = 1, \dots, M, \quad (7)$$

where M is the number of simulations. I tried to compute bond prices of the DSGE model in this paper using this method. However, I found that while linear coefficients stabilized as we increased M , nonlinear coefficients did not. Therefore, numerical approximation errors in bond prices may not be well controlled in this approach. Hence, there is merit in using closed form solutions suggested in this paper. In addition, the approximation of the integration operator in Euler equations by simulation contains an additional error term that is not present in my closed-form expressions for bond yields.¹

Hördahl et al. (2008) suggest an analytical way of approximating the conditional expectations for log bond prices in Euler equations. However, while they preserve some second-order terms, they ignore other second-order terms in the approximate log stochastic discount factor. For example, suppose a second-order approximation to the log stochastic discount factor after pruning results in $m_{t,t+1} = m_0 + m_1 x_t + x_t' m_2 x_t + m_3 \epsilon_{t+1} + x_t' m_4 \epsilon_{t+1} + \epsilon_{t+1}' m_5 \epsilon_{t+1}$. In Hördahl et al. (2008), the log price of the one period bond is computed by the mean and variance of the log stochastic discount factor as follows,

$$p_{1,t} = E_t(m_{t,t+1}) + \frac{V_t(m_{t,t+1})}{2}. \quad (8)$$

Since computing the variance of $m_{t,t+1}$ is complicated, they approximate the variance up to the second-order by using only first-order terms in $m_{t,t+1}$. Hence, they approximate $V_t(m_{t,t+1})$ by $m_3 V_t(\epsilon_{t+1}) m_3'$. While their approximation to the variance can be second-order accurate, their approximation to the log bond price ($\log E_t(e^{m_{t,t+1}})$) is not, in general, second-order accurate. When $m_{t,t+1}$ is a normal random variable, equation (8) computes the exact conditional expectation in the Euler equation; however, when $m_{t,t+1}$ is not a normal random variable, there is no guarantee that equation (8) is an accurate second-order approximation to $\log E_t(e^{m_{t,t+1}})$. In particular, terms like $x_t' m_4 \epsilon_{t+1}$ are ignored while terms like $\epsilon_{t+1}' m_5 \epsilon_{t+1}$ are considered. All these terms are equally second-order terms and affect the log bond price if the expectation in equation (8) is not approximated. Hence, given a second-order approximation to the stochastic discount factor, their method is less accurate for bond yields than the one suggested in this paper.

Rudebusch and Swanson (2008) suggest another way of obtaining closed form solutions for equilibrium bond yields. They compute the price of an infinitely lived consol which has the same

¹Binsbergen et. al. (2010) apply analytical approximation to conditional expectations by adding Euler equations for bond prices into the system of equations of the model. Since they apply a third order approximation to the solution of the model, the direct comparison of the approximation accuracy of bond prices is not possible. However, given a second-order approximation to equilibrium conditions, this method is less accurate than the one suggested in this paper.

duration as the long-term zero coupon bond. Since the consol price does not consider higher-order impacts such as convexity, the magnitude of approximation error implicit in this procedure can be hard to define precisely. In contrast, the approximation error of the method in this paper is tightly linked with the approximation accuracy of the solution. All the terms I throw away in the approximation are higher than second-order.

3 Measurement errors and particle filtering

The predictive error likelihood $p(z_t|z^{t-1}, \vartheta)$ can be evaluated by $\int \int p(z_t|x_t, \vartheta)p(x_t|x_{t-1}, \vartheta)p(x_{t-1}|z^{t-1}, \vartheta)dx_{t-1}dx_t$. In the linear and Gaussian world, the Kalman filter provides the analytical solution for the integral. In the general nonlinear model, it is no longer the case but I can approximate the integral by Monte Carlo methods. Particle filtering is one of these methods. The detailed description of the filtering step is available in Arulampalam et. al. (2002) and Doucet et. al. (2001). In this section, I will focus on why assumptions about measurement errors determine the smoothness of the approximation of the unknown filtering density. To simplify the exposition, consider the following univariate observed variable case with a single latent state variable,

$$\begin{aligned} x_t &= \Gamma(\vartheta)x_{t-1} + \sigma\eta\epsilon_t, \\ z_t &= \alpha_0(\vartheta) + \alpha_1(\vartheta)x_t + \alpha_2(\vartheta)x_t^2 + \xi_t \text{ where } \xi_t \sim \mathcal{N}(0, H). \end{aligned}$$

If H is equal to 0, there is no measurement error. In this case, the weight for the i_{th} particle is given by,

$$\pi_t^{a,i} = p(z_t|x_t^{a,i}, \vartheta) \begin{cases} 1, & \text{if } z_t = \alpha_0(\vartheta) + \alpha_1(\vartheta)x_t^{a,i} + \alpha_2(\vartheta)(x_t^{a,i})^2 \\ 0, & \text{otherwise.} \end{cases}$$

$\pi_t^{a,i}$ is sensitive to parameters (ϑ) and particles. Since the approximate likelihood is computed by the average of these weights over particles, it is also quite sensitive to the choice of particles.

Now, assume that H is positive. Then, $\pi_t^{a,i}$ is as follows,

$$\pi_t^{a,i} = \frac{K_H\left(\frac{z_t - \alpha_0(\vartheta) - \alpha_1(\vartheta)x_t^{a,i} - \alpha_2(\vartheta)(x_t^{a,i})^2}{\sqrt{H}}\right)}{\sqrt{H}}.$$

Here, K_H is a probability density function of a standard normal random variable. The resulting likelihood function takes the following form,

$$\mathcal{L}(\vartheta|z_t) = \frac{1}{N} \sum_{i=1}^N \pi_t^{a,i} = \frac{1}{N\sqrt{H}} \sum_{i=1}^N K_H\left(\frac{z_t - \alpha_0(\vartheta) - \alpha_1(\vartheta)x_t^{a,i} - \alpha_2(\vartheta)(x_t^{a,i})^2}{\sqrt{H}}\right).$$

The above expression shows that the standard deviation of the measurement error plays a similar role as the bandwidth in the kernel density estimator in which the Gaussian kernel is used.

Therefore, a too high (low) standard deviation of the measurement error implies oversmoothing (undersmoothing) of the likelihood approximation by particle filters.²

In the estimation of the nonlinear version of the DSGE model, I fixed standard deviations of measurement errors at 20% of sample standard deviations of observed variables. I tried alternative calibrations which set standard deviations of measurement errors at 10% and 40% of sample standard deviations of observed values. The estimation results including the bi-modality and the relative magnitude of the likelihood at each mode were essentially unchanged when I increased standard deviations of measurement errors; however, the numerical value of the likelihood gets smaller. On the other hand, the likelihood approximation was not reliable when we decreased the standard deviations of measurement errors.³ In addition, running MCMC chains to explore the posterior distributions of parameters turned out to be challenging with the low standard deviations of measurement errors because the likelihood was very rough due to undersmoothing. These results suggest that the baseline calibration provides a reasonable degree of smoothing.

4 MCMC algorithm

The random walk Metropolis-Hastings algorithm widely used in the estimation of DSGE models usually starts from the posterior mode. However, in the nonlinear model, finding the posterior mode by numerical optimization routines does not work well, since the particle filtering step introduces a discrete approximation that makes the likelihood non-smooth. An MCMC algorithm can be used as an optimization tool. Indeed, I find that even after a small number of draws I get to the point with a higher posterior density than the one reached by the simplex method. In addition, I update the proposal density based on the initial draws to fine tune the MCMC algorithm. This adaptation helps me to mitigate the possible inefficiency arising from not starting a MCMC chain at the posterior mode. The procedure works as follows,

- **Step 1 Selection of the Starting Point** : Compute the log-likelihood for 100 posterior draws in the linear model. Select one point which gives the highest log-likelihood value ϑ^* .
- **Step 2 Proposal** : Starting from ϑ^* , generate a new draw by the following random-walk proposal density,

$$\vartheta^{N,j+1} = \vartheta^j + c\mathcal{N}(0, I) , j = 0, \dots, R - 1.$$

The scaling matrix c is chosen by multiplying a small positive real number to the prior covariance matrix.

- **Step 3 Accept/Reject** Compute the acceptance rate $\alpha = \min\{\frac{p(\vartheta^{N,j+1}|z^T)}{p(\vartheta^j|z^T)}, 1\}$ and accept or reject $\vartheta^{N,j+1}$ according to the value of u which is drawn from the uniform distribution over the unit interval $[0, 1]$,

²However, having measurement errors does not guarantee the smoothness of the overall likelihood because I still use a discrete approximation to the filtering density when we draw particles to predict the next period values of observed variables.

³At the low standard deviations of measurement errors, the number of particles that contribute to the computation of the likelihood in a non-negligible way decreased by 90% compared to the baseline calibration. The depletion of the number of effective particles indicates that the value of the approximate likelihood will vary a lot depending on the number of particles used. Further details on results from alternative calibrations are available from the author upon request.

$$\vartheta^{j+1} = \begin{cases} \vartheta^{N,j+1}, & \text{if } u < \alpha \\ \vartheta^j, & \text{otherwise.} \end{cases}$$

Go back to step 2 and repeat.

- **Step 4 Updating the Scaling Matrix** After obtaining 100,000 draws in this manner, update the scaling matrix as a covariance matrix based on this output, and run a new MCMC chain, starting around the mean of the previous 100,000 draws with the updated scaling matrix. 50,000 draws from the new MCMC chain are used for the posterior inference in macro estimation. In the joint estimation, I use an independent Metropolis-Hastings algorithm to handle the bi-modality issue. Denote ϑ^i , ($i = 1, 2$) as the associated local mode in each area. Update the scaling matrix by the correlation matrix (c_i) based on 100,000 draws in each area. Start a new chain around one of ϑ^i 's and use the following mixture of t -densities as the proposal density,

$$\vartheta^{N,j+1} = 0.5t(\vartheta^1, c_1, df) + 0.5t(\vartheta^2, c_2, df), \quad j = 0, \dots, R-1.$$

Here, df stands for the degree of freedom which is 5 in this case. and I use 50,000 draws from the new chain for posterior inference. In linear models, I update the scaling matrix based on 1,000,000 draws and use 100,000 draws from the new chain for posterior inference.

5 Monte Carlo smoothing algorithm

The key steps of Monte Carlo smoothing can be described as follows:

- **Step 1** : Store resampled state variables x_t^i at each time for $i = 1, \dots, N$,
- **Step 2** : For $\{x_T^i\}_{i=1}^M$, calculate $w_{T-1|T}^{i,j} \propto p(x_T^i | x_{T-1}^j)$ where $M \leq N$,
- **Step 3** : Choose $x_{T-1}^k = x_{T-1}^j$ with probability $w_{T-1|T}^{i,j}$ for $k = 1, \dots, N$,
- **Step 4** : Repeat **Step 2** and **Step 3** until M trajectories of smoothed states $x_{1:T}$ conditional on z^T are obtained.

I follow Godsill et.al. (2004) and generate a substantial number of trajectories of state variables based on the resampled state variables in the forward filtering. Fernández-Villaverde and Rubio-Ramírez (2007) make the number of trajectories equal to the number of particles; however, since the computation time of one trajectory amounts to one evaluation of the likelihood, this is computationally costly. In a simulation study, 6,000 trajectories are enough to make the mean estimates close to true values. Smoothed estimates of macro factors in the paper are based on 6,000 trajectories of state variables.

6 The Posterior Mass of the Flexible Price Mode and Nonlinearities in the Model Solution

The posterior distributions of parameters in the paper show a noticeable difference between the linear model and the nonlinear model in terms of the posterior mass of the flexible price mode. In the linear model, the flexible price mode gets nearly zero posterior mass because the likelihood is substantially lower compared to the sticky price mode. However, in the nonlinear model, there is a small but positive posterior mass for the flexible price mode.

To determine if this difference comes from ignoring nonlinearities in macro dynamics or yield curve dynamics, I compare the model fit of each model evaluated at the flexible price mode of the nonlinear model. The model implied inflation and the five-year bond yield plotted together with actual data in Figures 1 and 2 suggest that ignoring nonlinearities in inflation dynamics generates much more volatile inflation than seen in data; however it does not deteriorate the fit for bond yields. Even at the linear model, a highly persistent inflation target shock can generate substantial variation of long-term bond yields through changes in long-run inflation expectations. However, in the linear model, these substantial variations of the long-run inflation expectations are directly linked with fluctuations of inflation and near-term inflation expectations. In contrast, in the nonlinear model, quadratic terms showing up in the policy function of inflation at least partially offset this linear effect. This mechanism will be clear if we take a look at the following policy function for inflation in the nonlinear model,

$$\pi_t = \frac{1}{2}g_{\sigma\sigma}^{\pi}\sigma^2 + g_{\pi}x_t + \frac{1}{2}x_t'g_{\pi\pi}x_t. \quad (9)$$

In the linear model, the volatility of π_t is proportional to the volatility of x_t ; however, if $g_{\pi\pi}$ is a negative definite matrix, the quadratic term may actually dampen the volatility of π_t when the volatility of x_t increases. At the flexible price mode, the component of $g_{\pi\pi}$ associated with the product of π_t^* and $\epsilon_{i,t}$ is significantly negative. This implies that a positive policy shock offsets the impact of high inflation target on inflation and near-term inflation expectations. At the same time, long-run inflation expectations can be still high because the highly persistent inflation target will be a dominant factor in the long run.

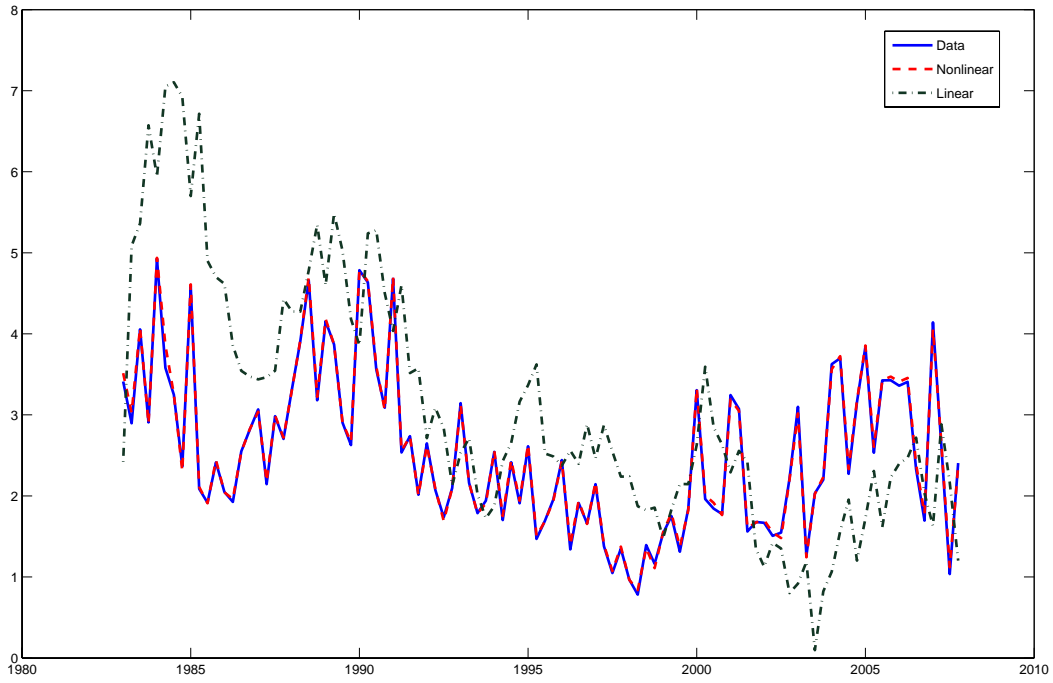
7 Estimation of the Linear Model with Survey Data

The differences in the correlation between the model-implied inflation expectations and survey-based inflation expectations across the flexible price mode and the sticky price mode suggest that including survey data in the estimation may change the likelihood of the two modes. While estimating the nonlinear model with survey data is too onerous, because I have to compute inflation expectations by simulation for each particle used, the estimation of the linear model is not. Estimation results of the linear model with the dataset augmented by survey data on 1-year ahead inflation expectations are provided in Table 1. We still find the bi-modality of parameters in this case; however, the probability mass of each mode changes a lot. While the likelihood of the flexible price mode was much lower without survey data, now it has a higher likelihood.

Additional References

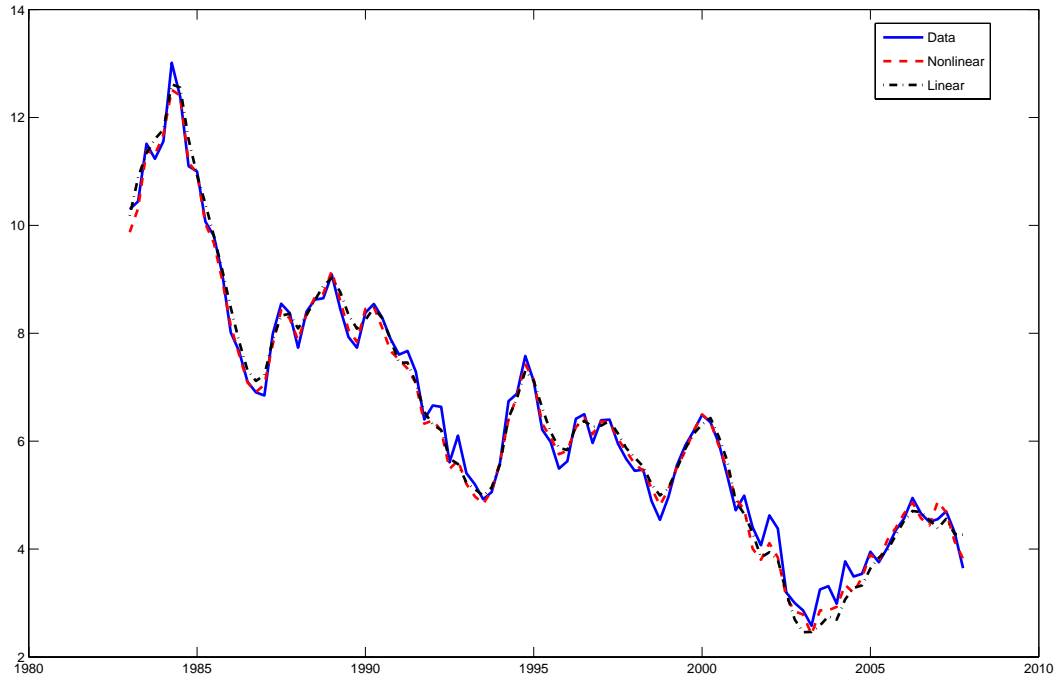
- Arulampalam, M. S., S. Maskell, N. Gordon, and T. Clapp (2002): "A Tutorial on Particle Filters for Online Nonlinear/Non-Gaussian Bayesian Tracking," *IEEE Transactions on Signal Processing*, **50**(2), 173-188.
- Doucet, A., J.F.G. De Freitas, and N.J. Gordon (2001): *Sequential Monte Carlo Methods in Practice* New York, NY: Springer-Verlag.

Figure 1: FIT FOR INFLATION AT THE FLEXIBLE PRICE MODE



Notes: Fitted values are obtained by using both the linear and the nonlinear solutions at the flexible price mode of the nonlinear model.

Figure 2: FIT FOR 5-YEAR BOND YIELD AT THE FLEXIBLE PRICE MODE



Notes: Fitted values are obtained by using both the linear and the nonlinear solutions at the flexible price mode of the nonlinear model.

Table 1: LOCAL MODES OF THE POSTERIOR DENSITY: LINEAR MODEL WITH SURVEY DATA

| Parameter | Flexible price mode | Sticky price mode |
|----------------------|---------------------|-------------------|
| τ | 0.51 | 4.48 |
| β | 0.999 | 0.995 |
| $\ln f^*$ | 0.346 | 0.083 |
| ϕ | 29.16 | 72.43 |
| $400u_a^*$ | 2.44 | 2.04 |
| γ_p | 3.00 | 2.19 |
| γ_y | 0.118 | 0.123 |
| ρ_a | 0.950 | 0.253 |
| ρ_f | 0.968 | 0.973 |
| ρ_i | 0.874 | 0.509 |
| ρ_{π^*} | 0.997 | 0.786 |
| $400\eta_a$ | 0.72 | 3.08 |
| $100\eta_f$ | 2.58 | 3.06 |
| $400\eta_i$ | 0.68 | 0.8 |
| $400\eta_{\pi^*}$ | 0.36 | 0.4 |
| $\ln A_0$ | 9.7239 | 9.7961 |
| $400 \ln \pi^*$ | 3.12 | 5.64 |
| h | 0.7817 | 0.3825 |
| log posterior kernel | 4,534.3 | 4,503.5 |
| (log likelihood) | 4,580.7 | 4,487.5 |

Notes: Survey data on expected inflation as well as macro and term structure data are used for the estimation of the model.